The role of nucleon knockout in pre-equilibrium reactions

E.V. Chimanski[1,2], *B.V. Carlson*[1], *R. Capote*[2], *A.J. Koning*[2]
[1]Aeronautics Institute of Technology, São José dos Campos, Brazil
[2]NAPC-Nuclear Data Section, International Atomic Energy Agency, Vienna, Austria

Abstract
Nucleon-induced pre-equilibrium reactions are predominantly direct reactions. At low incident energies, excitation of all but the lowest energy collective states can be well described in terms of one-step reactions that produce particle-hole pairs. As the incident energy increases, the probability of exciting a nucleon to the continuum rather than to a bound particle state also increases. These knockout nucleons can escape the nucleus or induce secondary collisions that create still other continuum or bound particle-hole pairs. We discuss their role in precompound nuclear reactions here.

1 Introduction

Above an incident energy of about 20 MeV, nucleon-induced pre-equilibrium reactions are dominated by direct reactions. Excitation of all but the lowest energy collective states can be well described in terms of one-step reactions that produce particle-hole pairs for smaller incident energies in this range. As the incident energy is increased, more complex excitations involving two or more particle-hole pairs become accessible through multi-step reactions. Quantum mechanical models of such multi-step direct reactions were developed many years ago [1–3] and have been studied and improved many times over since then [4–7]. In these models, a leading continuum particle initiates the reaction and remains in the continuum as it scatters repeatedly from the nucleus to produce successive particle-hole pairs. However, as the incident energy increases, the probability of exciting a nucleon to the continuum rather than to a bound particle state also increases [8]. These knockout nucleons can escape the nucleus or induce secondary collisions that create still other continuum or bound particle-hole pairs. They are not taken into account in the MSD models developed until now.

The calculation of knockout to the continuum is a relatively straightforward extension of actual MSD calculations. However, here we would like to obtain a more general idea of the importance of this mechanism in pre-equilibrium reactions. This would require an extension of the existing MSD models codes to an arbitrary number of interactions leading to both bound and continuum configurations. As this is unfeasible, we will make use of the semiclassical DDHMS pre-equilibrium simulation model of Blann and Chadwick [9, 10]. As well as being the most conceptually sound semiclassical model, it is also the closest in correspondence to the quantum mechanical MSD models.

2 Method

An important characteristic of nucleon-induced pre-equilibrium reactions is that their early stages are dominated by collisions that increase the number of particle-hole pairs [3, 11]. This implies that the equal occupation of states with the same particle-hole number, assumed in the semiclassical exciton and hybrid models, is not justified. This limits their applicability to low energies, for which configurations above the two particle - one hole one are not extremely important.

As an alternative, Blann proposed the "hybrid Monte Carlo simulation" (HMS) model [9], in which a sequence of independent particle-hole pairs is excited during a reaction. Each excited particle and hole is considered an independent degree of freedom. Particles can be emitted and particles and holes with sufficient energy can create subsequent particle-hole pairs. Emission occurs in accord with the particle emission widths and excitation in accord with the particle and hole damping widths. At each step of the

Monte Carlo simulation, an emission or particle-hole excitation is chosen based on the relative weight of the widths. The process continues until no particle or hole possesses sufficient energy to be emitted or to excite another particle-hole pair. Blann and Chadwick later extended the model to the DDHMS one, which calculates angular distributions as well as spectra [10].

While the equal occupation assumption of the exciton and hybrid models requires a strong residual interaction between states with the same particle-hole number, the independent particle and hole modes of the HMS model require that there be no residual interaction at all. Comparisons with complete simulations performed using an interaction consistent with the shell model show the HMS model to provide excellent agreement with the more complete calulations while the exciton model does not [12].

Since all active particles and holes can be followed in an HMS calculation, we can tag them according to the number of collisions that have occured. Collision 1 is induced by the incident particle and initially labels this particle as well as the particle-hole pair it produces. Collision 2 is induced by one of these three and labels it as well as the particle-hole pair produced. The labelling continues for higher collison numbers.

The average number of collisons before formation of a residual compound nucleus is quite small on the average, as can be seen in Fig. 1, where, for a proton incident on ^{58}Ni, it increases from a value of about two at 10 MeV to about four at 200 MeV. The standard deviation also grows slowly, from a value of about one at 10 MeV to about three at 200 MeV. Interestingly, the difference between the average value and the standard deviation appears to be fixed at a value of one at all energies. In contrast, the maximum number of collisions before compound nucleus formation grows approximately linearly with the energy and reaches a value close to 50 at 200 MeV.

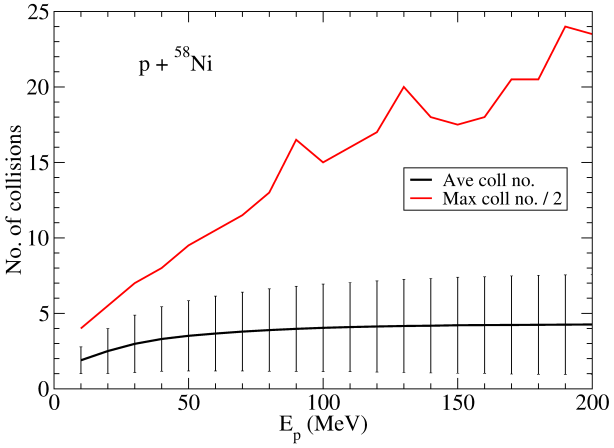

Fig. 1: Average and total number of collisions before compound nucleus formation for the collision $p + {}^{58}$Ni

We label the emited particles according to their collision numbers as follows:

- **inel** - particles emitted after one collision in which the second particle is in a bound state;
- **ko** - particles emitted after one collision in which the second particle is also emitted;
- **1** - particles emitted after on collision independently of hat happens to the collision partner;
- **2** - particles emitted after two collisions (although the second collision might be the emitted particles first collision) independently of what happens to the collision partner;
- **all** - particles emitted after any number of collisions.

The particles labelled **inel** correspond most closely to the leading particle of a usual one-step MSD reaction. In all cases, the residual nucleus might still emit other particles.

3 Results

To relate our calculations to experimental data, we compare our inclusive proton and neutron emission spectra for 90 MeV proton-induced reactions with the data of Refs. [13] and [14]. Our calculations were obtained using the HMS module in the EMPIRE-3 neutron reaction code [15]. All pre-equilibrium and compound nucleus emission has been taken into account. The quasi-elastic peak has not been included.

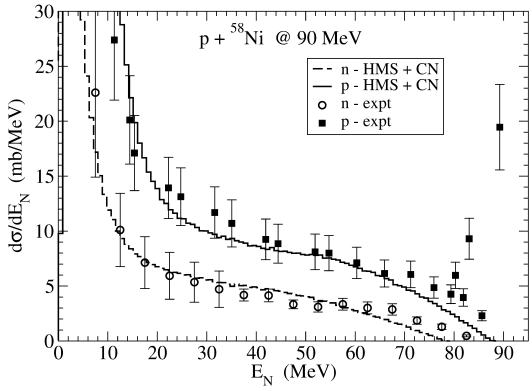

Fig. 2: Calculated inclusive neutron and proton emission spectra compared with the experimental data of Refs. [13] and [14] for the collision $p + {}^{58}$Ni.

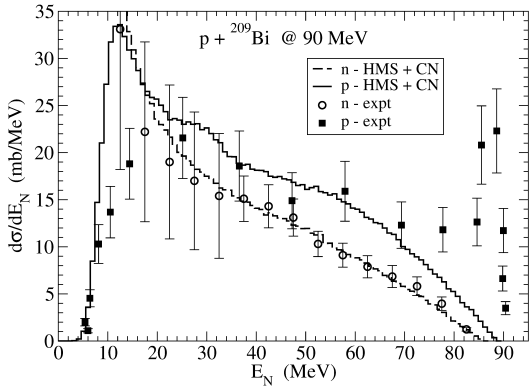

Fig. 3: Calculated inclusive neutron and proton emission spectra compared with the experimental data of Refs. [13] and [14] for the collision $p + {}^{209}$Bi.

In Figs. 2 and 3, we display the calculated inclusive emission spectra for ^{58}Ni and ^{209}Bi together with the experimental data. The agreement between the two is quite good, except for the lower energy proton emission from ^{209}Bi, which is overestimated by the calculations.

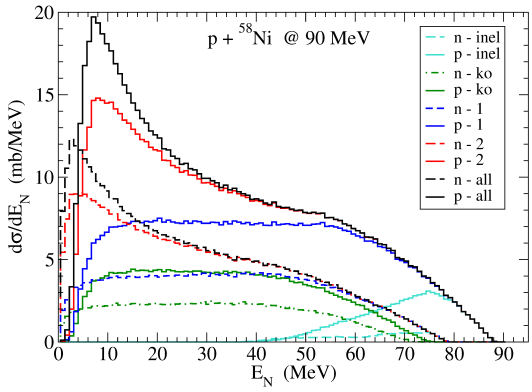

Fig. 4: Contributions to the inclusive nucleon emisson cross sections from the collision $p + {}^{56}$Ni.

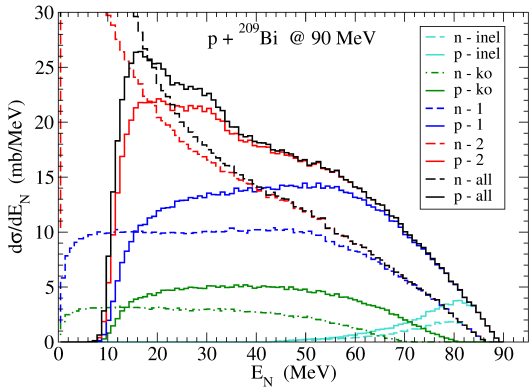

Fig. 5: Contributions to the inclusive nucleon emisson cross sections from the collision $p + {}^{209}$Bi.

In Figs. 4 and 5, we show the decomposition of the inclusive emission cross spectra for ^{58}Ni and ^{209}Bi into their inelastic (inel), knockout (ko), first collision (1) and second collision (2) components. We observe that the emissions resulting in inelastic excitation exhaust the emission spectra for only a small range of about 10 MeV of the most energetic emissions. They then fall slowly, reaching zero at an energy corresponding to an excitation of the residual nucleus of about 50 MeV. Each of the first emission spectra minus the corresponding inelastic spectrum increases roughly in parallel with the corresponding knockout spectrum as the emission energy is reduced from its maximum value. The first emission and knockout spectra saturate at an energy corresponding to an excitation of the residual nucleus of about 25 to 30 MeV and remain flat until decreasing to zero at the Coulomb barrier for protons and at zero energy for neutrons. Finally, we observe that the particles emitted after at most two collisons (2) exhaust

the spectra except at very low excitation energies. As we have seen in Fig. 1, the average number of collisons at 90 Mev is between three and four. We can thus conclude, to a good approximation, that the collisions beyond the first two lead on the average to the formation and subsequent decay of a compound nucleus.

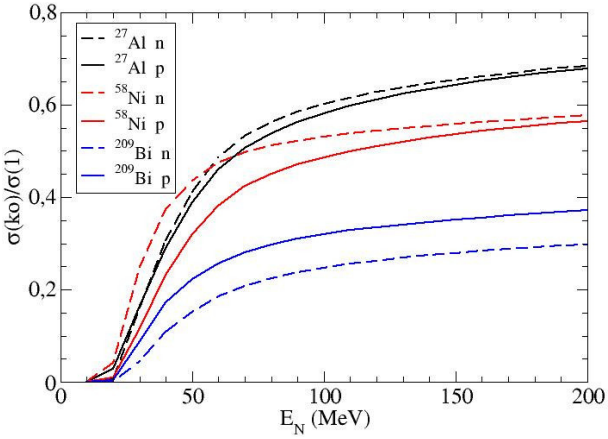

Fig. 6: Ratio of knockout to one interaction neutron and proton emission cross sections for p + ^{27}Al, ^{58}Ni and ^{209}Bi.

The similar behavior of the knockout and first emission spectra as a function of energy suggests a simple relation between the two. The definitions of the two types of emissions also suggest such a relation: in knockout, both nucleons leave the nucleus after only one collision, while in first collison emission, the emitted nucleon suffers only one collision. The difference betwen the two thus refers to the first collisions in which the second nucleon suffers a second collison (or more) before escaping. Since the number of collisions a nucleon participates in is roughly proportional to the nuclear matter through which it passes, we can associate knockout emission with superficial collisions with the target and the remaining first emission nucleons with more central collisions. The simplest estimate we might make is that the knockout cross section should be restricted to an outer ring of width ΔR of the total first emission cross section πR^2. We would then have for the ratio

$$\sigma(ko)/\sigma(1) = (\pi R^2 - \pi(R - \Delta R)^2)/\pi R^2 = 1 - (1 - \Delta R/R)^2.$$

We plot the ratio of the two cross sections as a function of the incident energy for three nuclei: ^{27}Al, ^{58}Ni and ^{209}Bi in Fig. 6. We observe that the ratios for neutron and proton knockout are very similar for each nucleus. The ratios increase fairly rapidly below about 50 MeV, in the region of excitation energy in which inelastic excitation still contributes, and much more slowly above. The ratios decrease with increasing mass of the target nucleus as would be expected from the discussion above.

Table 1: Average ratio of knockout to first emission cross sections at 200 MeV and the corresponding effective surface thickness ΔR for the given nuclei.

Nucleus	Ratio	ΔR (fm)
^{27}Al	0.7	1.7
^{58}Ni	0.55	1.6
^{209}Bi	0.35	1.4

In the table, we give an estimate of the cross section ratio at an incident energy of 200 MeV and of the ring thickness ΔR in which knockout dominates. We observe that the value of ΔR is not constant

but decreases slowly as the mass number of the nucleus increases. We argue that this does not invalidate the interpretation but simply reflects the increasing thickness of the matter that must be traversed as the mass number increases.

4 Conclusions

Nucleon-induced pre-equilibrium reactions are dominated by direct reactions. Quantum mechanical multi-step direct models of these reactions have treated them as being exclusively inelastic excitations. Using the semiclassical HMS model, we have shown here that nucleon knockout - direct excitation to the continuum - makes an important contribution to the emission cross section at incident energies above about 20 to 30 MeV. We are currently working to extend the quantum mechanical MSD model to explicitly include these reactions.

Acknowledgements

EVC acknowledges financial support from grants 2016/07398-8 and 2017/13693-5 of the São Paulo Research Foundation (FAPESP). BVC acknowledges financial support from grant 2017/05660-0 of the São Paulo Research Foundation (FAPESP) and grant 306433/2017-6 of CNPq. EVC and BVC acknowledge support from the INCT-FNA project 464898/2014-5.

References

[1] H. Feshbach, A. Kerman, S. Koonin, Ann. Phys (N.Y.). 125 (1980) 429.

[2] T. Tamura, T. Udagawa, H. Lenske, Phys. Rev. C 26 (1982) 379.

[3] H. Nishioka, H. A. Weidenmüller, S. Yoshida, Ann. Phys. (N.Y.) 183 (1988) 166.

[4] A. Koning, M. Chadwick, Phys. Rev. C 56 (1997) 970.

[5] T. Kawano, S. Yoshida, Phys. Rev. C 64 (2001) 024603.

[6] M. Dupuis, T. Kawano, J. P Delaroche, E. Bauge, Phys. Rev. C 83 (2011) 014602.

[7] M. Dupuis, E. Bauge, S. Hilaire, S. F. Lechaftois, S. Péru, N. Pillet, C. Robin, Eur. Phys. J. A 51 (2015) 168.

[8] B. V. Carlson, J. E. Escher, M. S. Hussein, 41 (2014) 094003.

[9] M. Blann, Phys. Rev. C 54 (1996) 1341.

[10] M. Blann, M. Chadwick, Phys. Rev. C 57 (1998) 233.

[11] J. Bisplinghoff, Phys. Rev. C 33 (1986) 1569.

[12] C. A. Pompeia, B.V. Carlson, Phys. Rev. C 74 (2006) 054609.

[13] J. R. Wu, C. C. Chang, H. D. Holmgren, Phys. Rev. C 19 (1973) 698.

[14] A. M. Kalend, B. D. Anderson, A. R. Baldwin, R. Madey, J. W. Watson, C. C. Chang, H. D. Holmgren, R. W. Koontz, J. R. Wu, and H. Machner, Phys. Rev. C 28 (1983) 105.

[15] M. Herman, R. Capote, B. V. Carlson, P. Oblozinský, M. Sin, A. Trkov, H. Wienke, V. Zerkin, Nuclear Data Sheets 108 (2007) 2655.